

## Event and conditions that produced the iron meteorite Block Island on Mars

John E. Chappelow<sup>1</sup> and Matthew P. Golombek<sup>2</sup>

Received 29 May 2010; accepted 14 July 2010; published 4 November 2010.

[1] The Mars Exploration Rover Opportunity has discovered four large iron-nickel meteorites that range in size from 50 to 240 kg dispersed over 10 km of Meridiani Planum, Mars. Because these meteorites are covered with hollows that resemble regmaglypts, their surfaces record their ablation through the atmosphere, and they must have landed at speeds below hypervelocity ( $<2 \text{ km s}^{-1}$ ) to survive. Slowing massive iron meteorites requires a minimum atmospheric density, which was quantified using a numerical model that integrates the equations of motion for incoming meteoroids through an atmosphere of a given surface density and scale height and records their outcomes as direct (generally hypervelocity impacts that form craters), longer over the horizon and fallback flight paths, and skip outs. The present atmosphere of Mars is sufficient to slow iron meteoroids as large as Block Island (the most massive meteorite) via drag and significant ablation on long flight paths, although for standard distributions of entering meteoroid masses, velocities, and entry angles, such events are rare (0.007% of incoming iron meteoroids). Such events require entry angles of  $10^\circ$ – $13^\circ$ , entry velocities of  $6$ – $18 \text{ km s}^{-1}$ , and entry masses of  $225$ – $710 \text{ kg}$ . The absence of large stony meteorites is probably at least partially because they are much weaker and thus broken up into smaller fragments on impact. Although differential drag deceleration on long flight paths could disperse fragments of an entering meteoroid by tens of kilometers, dynamic pressures are too low to break up an iron meteorite, leaving the possibility that they are paired an open question.

**Citation:** Chappelow, J. E., and M. P. Golombek (2010), Event and conditions that produced the iron meteorite Block Island on Mars, *J. Geophys. Res.*, 115, E00F07, doi:10.1029/2010JE003666.

### 1. Introduction

[2] In the absence of an atmosphere, meteoroids encountering a planet strike its surface at speeds given by a combination of their “cosmic” velocities relative to the planet and the planet’s escape velocity. The escape velocity itself is the theoretical minimum for impact, which for Mars is  $\sim 5 \text{ km s}^{-1}$ , and is only possible for objects that are essentially coorbital with the planet. Their impact velocities are therefore of the order of kilometers or tens of kilometers per second, and they are almost completely destroyed by pulverization, melting, and vaporization in such hypervelocity impacts. Relatively intact meteorites are only produced if the planet has an atmosphere dense enough to decelerate them sufficiently, via aerodynamic drag and ablation, to survive impact.

[3] For objects encountering Mars, with aphelia in the asteroid belt, their impact velocities would be given by the limiting values

$$\nu_{\min} = \left[ (\nu_{\text{obj}} - \nu_{\text{mars}})^2 + \nu_{\text{esc}}^2 \right]^{1/2}$$

for orbits with perihelia at Mars’ orbit and

$$\nu_{\max} = \left[ \nu_{\text{obj}}^2 + \nu_{\text{Mars}}^2 + \nu_{\text{esc}}^2 \right]^{1/2}$$

for objects with perihelia at the Sun, both for prograde heliocentric orbits. Here  $\nu_{\text{mars}}$  is Mars’ orbital velocity,  $\nu_{\text{obj}}$  is the velocity of the Mars-crossing object at Mars’ orbital distance, and  $\nu_{\text{esc}}$  is Mars’ escape velocity. For Mars these numbers are  $\nu_{\min} = \sim 6 \text{ km s}^{-1}$  and  $\nu_{\max} = \sim 31 \text{ km s}^{-1}$  [see Chappelow and Sharpton, 2005], with a mean value of about  $11 \text{ km s}^{-1}$  [e.g., Davis, 1993]. For objects whose aphelia may be between Mars’ orbit and the asteroid belt, the lower limit may be slightly less, but the absolute minimum for any Mars-impacting meteoroid is Mars’ escape velocity of about  $5 \text{ km s}^{-1}$ , and this value would only hold for objects that are in nearly the same orbit as Mars itself.

[4] Thus, without its atmosphere to slow them, meteoroids incident on Mars would be annihilated in hypervelocity impacts with the surface of at least several kilometers per second, regardless of their masses, preencounter velocities, or incidence angles. They would leave craters on the surface, but not meteorites in the usual sense, at least not the large and apparently intact ones that have now been found

<sup>1</sup>SAGA Inc., Fairbanks, Alaska, USA.

<sup>2</sup>Jet Propulsion Laboratory, California Institute of Technology, Pasadena, California, USA.

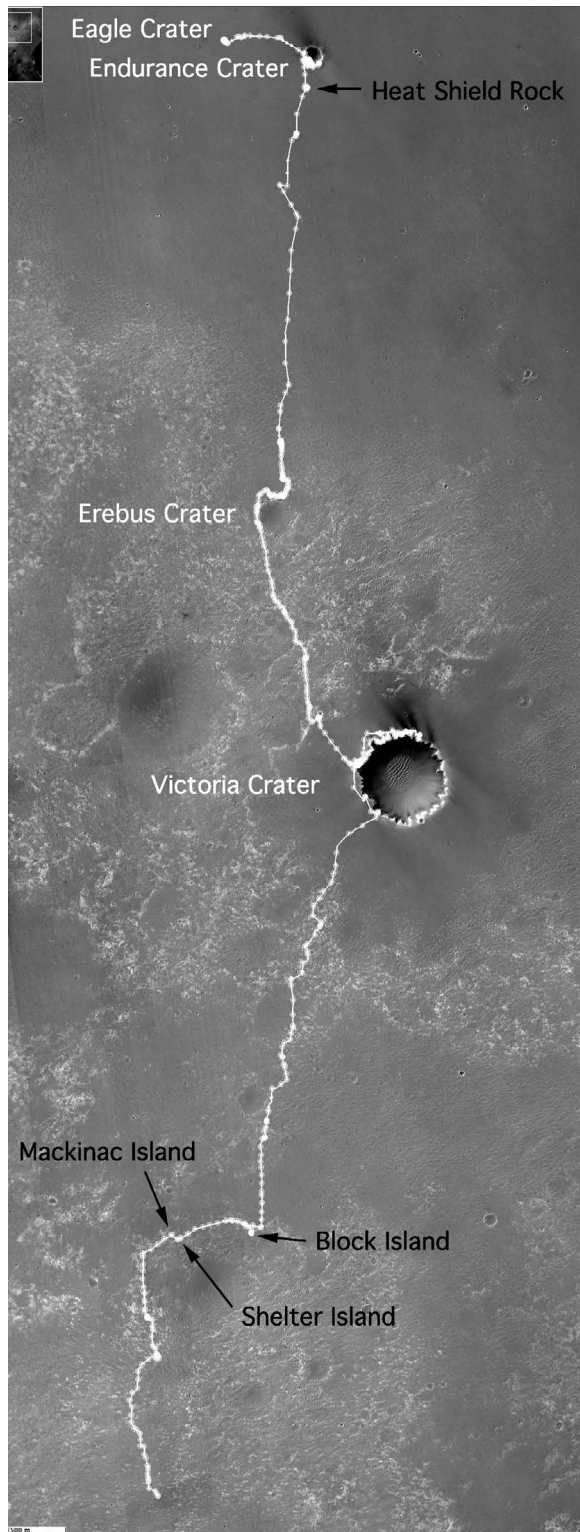


**Figure 1a.** High Resolution Imaging Science Experiment (HiRISE) image showing Opportunity traverse, iron meteorites (black), and a few craters (white) on Meridiani Planum. Traverse shown through sol 2218 of Opportunity's mission. Opportunity was at Heat Shield Rock on sols 344–351, Block Island on sols 1959–2009, Shelter Island on sols 2022–2035, and Mackinac Island on sols 2035–2038. HiRISE image PSP\_009141\_1780 is at 25 cm/pixel with north up.

on Mars. In this manner, the atmosphere modulates the production of meteorites and impact craters on the surface, depending upon the atmospheric density [Vasavada *et al.*, 1993; Chappelow and Sharpton, 2005, 2006a].

[5] Of course the decelerating effect of Mars' atmosphere also depends on the properties (e.g., mass distribution, densities) and entry conditions of the incident projectile population. For any given atmospheric density, there are limits to the masses of objects that can be slowed enough to survive impact, the flight paths they must follow, and their rates of accumulation on the surface. This relationship between an atmosphere and the impactor population passing through it can be exploited to predict the properties of the meteorite populations (e.g., mass distributions and compositions) that would be expected to be found on the surface [Bland and Smith, 2000; Chappelow and Sharpton, 2006a]. Conversely, given certain knowledge about the meteorite population, it can be used to investigate the atmosphere itself, the details of the meteorite-producing events, and even the properties of the original preatmospheric meteoroid population. In particular, the mass and physical properties of a given meteorite can be used to estimate limits on its atmospheric entry conditions and to estimate the minimum atmospheric density required to decelerate it down to a survivable impact speed [Chappelow and Sharpton, 2006b]. Paige *et al.* [2007] used the rovers observed lack of centimeter-size craters in a similar manner to constrain the minimum atmospheric density during expected recent obliquity cycles.

[6] Chappelow and Sharpton [2005, 2006a] found that Mars' current atmosphere (~6 mbar of average surface pressure) is too thin to slow the vast majority of iron or stony meteoroids more massive than ~1 kg enough to survive impact intact, as they still reach the surface at several kilometers per second. It thus came as somewhat of a surprise when in January 2005 the Mars Exploration Rover (MER) Opportunity found an approximately 50–60 kg iron meteorite, initially dubbed "Heat Shield Rock" (HSR) but later renamed Meridiani Planum after its place of discovery (Figures 1a and 1b). Speculation at the time ran toward the possibility that Mars must have had a denser atmosphere when HSR landed since, in addition to its large mass, the high density implied by its composition [Morris *et al.*, 2006] (kamacite: ~7900 kg m<sup>-3</sup> [Roberts *et al.*, 1990]) would make it difficult for the atmosphere to decelerate. However, Chappelow and Sharpton [2006b] showed that, given certain specific entry conditions, HSR *could* be accounted for, even under current martian atmospheric conditions.

[7] More recently, MER Opportunity has discovered three more large iron meteorites ~9.7 km south of HSR (Figure 1). Two of these are even larger than HSR, and therefore reopen the question of whether Mars must have had a denser atmosphere in the past in order to explain them. Beech and Coulson [2010] concluded that massive iron meteorites (>800 kg) would require an atmosphere at least one to two orders of magnitude denser than at present. Finally, the discovery of several such large iron meteorites with similar composition, which should be very rare compared to other meteorites on Mars, in such close proximity raises the possibility that they represent a strewn field produced by a

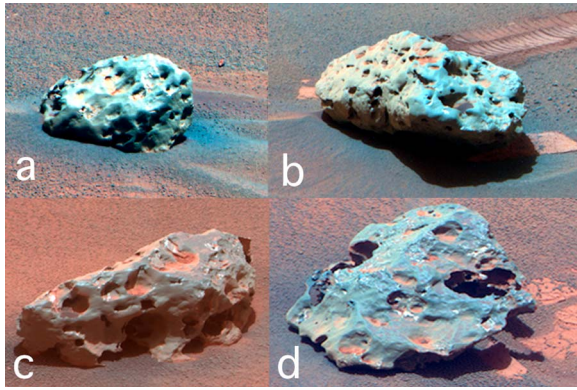


**Figure 1b.** Pancam color images of four iron meteorites discovered by Opportunity at Meridiani Planum. Note smooth surfaces with hollows that are interpreted as regmaglypts that form from ablation as the meteorite passes through the atmosphere. Preservation of regmaglypts indicates the meteorites were landed on the surface at much lower speed than hypervelocity impacts that form craters and are not spallation fragments from impacts. (a) Heat Shield Rock viewed from the east is about 30 cm across. (b) Block Island viewed from the southeast is about 60 cm across. (c) Shelter Island viewed from the east is about 50 cm across. (d) Mackinac Island viewed from the north-east is about 36 cm across.

single event. These and other questions are the subject of this study.

## 2. Heat Shield Rock

[8] Discovered over 5 years ago, the presence of HSR seemed at first to defy explanation in view of its high mass and density and the low density of the current martian atmosphere. It is rounded and covered with pits and hollows interpreted as ablation features (regmaglypts), with no sign of planar or angular features that would be indicative of fracture, and is therefore very unlikely to be a fragment or spall produced by the impact of a larger object. Nor does it seem likely to be a fragment of an object which broke apart in the atmosphere; if it fragmented low in the atmosphere there would be insufficient time for extensive regmaglypts to form, while higher up it would encounter only very weak dynamic pressures.

[9] And yet, if considered a single unfragmented object, a simple “air column” model of meteor deceleration [e.g., Melosh, 1989] completely fails to explain HSR’s presence, or the presence of any iron meteorites more massive, under current atmospheric conditions. Under such a model, HSR should have struck the surface at several kilometers per second, yet it does not show any signs of impact damage or deformation. When HSR was discovered, these facts taken together led to the speculation that Mars must once have had a denser atmosphere.

[10] However, quantitative study of the event that landed HSR soon established that this is not necessarily the case. Given a long enough flight path through the atmosphere,

Chappelow and Sharpton [2006b] found that the combination of aerodynamic drag and ablation could in fact land HSR on the surface at low enough speed to survive impact without significant damage. Such a trajectory would require very specific entry conditions, including a very narrow and shallow entry angle corridor, making the event quite unusual. But it would account for HSR, without the need to invoke a past, denser atmosphere. Unfortunately, the ranges of initial conditions explored in Chappelow and Sharpton [2006b] were incomplete, and therefore so are the results. That work is redone here using the full ranges of possible entry conditions, and the results are presented below.

## 3. New Discoveries: Block, Shelter, and Mackinac Islands

[11] Recently (July–October 2009), the MER Opportunity rover discovered three more iron meteorites on Meridiani Planum, two of them more massive than HSR: “Block Island” (BI), “Shelter Island” (SI), and “Mackinac Island” (MI); Block and Shelter Islands are nickel-iron (kamacite) meteorites, and Mackinac Island appears the same in images. Like HSR, two of the three (BI and SI) have been classified IAB iron meteorites [Schröder et al., 2008; Fleischer et al., 2010a; R. Gellert et al., APXS on iron nickel meteorites at Meridiani Planum, Mars, submitted to *Journal of Geophysical Research*, 2010]. At approximately five times the mass of HSR, Block Island in particular reopens the possibility that Mars once had a denser atmosphere.

[12] Meteorite masses were obtained by estimating their volumes using careful measurements of their dimensions, taken from Opportunity Navigation Camera (Navcam) images, then multiplying these by the density of kamacite. Stereo ranging errors for Navcam images have been measured as 1% of the distance to the target [Maki et al., 2003], suggesting uncertainties of about 1–3 cm for measurements from typical standoff distances of about 1–3 m. For Block Island, Navcam stereo images from six locations surrounding the rock were used by the Jet Propulsion Laboratory image processing group (the Multi-mission Instrument Processing Laboratory) to generate a three-dimensional shape model (J. W. Ashley et al., Evidence for mechanical and chemical alteration of three new iron-nickel meteorites on Mars: Process insights for Meridiani Planum, submitted to *Journal of Geophysical Research*, 2010), whose volume is close to that expected for a triaxial ellipsoid ( $4\pi l \times w \times h/3$ ), where  $l$ ,  $w$ , and  $h$  are one half the measured length, width, and height, respectively (R. Deen et al., private communication, 2010). Because these are iron meteorites of composition similar to kamacite we assumed a density of  $7900 \text{ kg m}^{-3}$ . Results are shown in Table 1 and indicate masses of 50, 65, 100, and 240 kg for HSR, MI, SI, and BI, respectively.

[13] Observations of these meteorites made by Opportunity [Fleischer et al., 2010a; Johnson et al., 2010; Ashley et al., submitted manuscript, 2010] show that all of them, like HSR, are mostly smooth with ubiquitous hollows, which are probably regmaglypts formed by ablation during passage through the atmosphere. With the exception of a small area on BI, none of them have any features that suggest fracturing or mechanical deformation. These observations argue that the meteorites are not spall or impact fragments from a larger impactor, because such fragments

**Table 1.** Measurements, Volumes and Masses of Iron Meteorites on Mars

Meteorite	Length (cm)	Width (cm)	Height (cm)	Volume (cm <sup>3</sup> )	Mass (kg)
Heat Shield Rock	30	30	14	6597	~50
Shelter Island	50	24	20	12,566	~100
Mackinac Island	36	26	17	8332	~65
Block Island <sup>a</sup>				30,429	240
Block Island <sup>b</sup>	60	40	25	31,416	

<sup>a</sup>From MIPL three-dimensional shape model.

<sup>b</sup>Dimensions measured.

would have surfaces dominated by fracture planes and broken edges. However, despite the absence of fracture features, we will show that it is possible that they could be fragments of a single object that broke apart in the atmosphere. This issue is addressed further below.

[14] As the largest meteorite yet discovered on Mars, BI would set a lower limit to the martian atmospheric density at the time of its arrival, if indeed a denser atmosphere is required. Therefore, this work focuses on the entry and atmospheric conditions required to produce Block Island.

#### 4. Methods

[15] Many of the methods used here are described in detail elsewhere [Chappelow and Sharpton, 2006a, 2006b], so only a summary of those methods is given here, except where necessary.

[16] The basic procedure is built around a numerical model of meteoroid passage through an atmosphere. The model uses a fourth-order Runge-Kutta routine to integrate the equations of motion of a single meteoroid’s passage through atmosphere, from atmospheric entry (assumed to occur at 100 km or ~9 atmospheric scale heights) to contact with the surface, or some other outcome. The atmosphere is modeled as a simple exponential in density versus altitude, with a specified surface pressure and scale height. The scale height is 10.9 km, and the density of the atmosphere can be changed by varying the density at the surface. After each integration step the simulation checks whether the test object has escaped the planet, ablated away, or struck the surface. If any of these has occurred the program stores all relevant information, including the outcome and the maximum dynamic pressure encountered, and moves on to the next test object. In this way this simulation is “scanned” over the ranges of interest in the entry parameters (entry mass ( $m_o$ ), velocity ( $\nu_o$ ), and angle ( $\theta_o$ )).

[17] The process begins with a low-resolution run of the program, covering the full possible ranges of  $m_o$ ,  $\nu_o$ , and  $\theta_o$ , in order to roughly estimate the ranges in these parameters that may result in HSR- or BI-like meteorites. This is repeated as necessary to reduce these ranges of interest as much as possible, and then a final, high-density run over the remaining parameter space of interest is performed. Once the integrations are complete, the BI- and HSR-like outcomes are sorted out of the results as follows.

[18] The outcomes are classified into three general categories: ablative mass loss to below 50 kg (denoted 0 on Figure 2), impact with the surface (denoted 1, 2, and 3 on Figure 2), and escape from the atmosphere and Mars

(denoted 4 on Figure 2). Trajectories that end with impacts on the surface are further differentiated because their frequencies of occurrence, dynamics, path lengths, times of flight, and likelihood to produce meteorites all differ dramatically. In order, they are referred to here as (1) “direct,” (2) “over the horizon,” and (3) “fallback” flight paths. Types 2 and 3 are far longer, in both arc length and time of flight, than type 1 and are therefore much more favorable for the production of large meteorites; indeed, beyond some mass limit, *only* these types can result in meteorites. But they also require quite improbable entry conditions, especially in terms of entry angle. Objects following these trajectories impact the surface beyond the horizon (H on Figure 2) as viewed from the starting point at 100 km altitude, approximately following the curvature of the planet as they descend. Type 3 is further distinguished as these objects actually regain altitude before falling back to the surface (Figure 3).

[19] Finally, the BI- and HSR-like outcomes are sorted out of the results. A result is considered BI-like if it impacts the surface with a velocity less than  $2 \text{ km s}^{-1}$  [Chappelow and Sharpton, 2006a] and with a final mass within about 10% of BI’s apparent mass,  $240 \pm 25 \text{ kg}$ .

[20] Each test object is also associated with a weight factor that is based on probability distributions in initial mass, entry velocity, and entry angle, measured downward from local horizontal (Figure 4). The defining distribution functions are described in detail in Chappelow and Sharpton [2005, 2006a] and are displayed in Figure 4. These are used to estimate the relative frequencies of the various sets of initial conditions ( $m_o$ ,  $\nu_o$ ,  $\theta_o$ ) and their outcomes. For example, they are used to estimate the relative contribution that each set of initial conditions makes to the martian population of BIs. For example, the fraction of Mars-incident test meteoroids that share any given outcome (such as BI-like meteorite) is simply the sum of the weight factors associated with that outcome.

[21] It is worth mentioning at this point that the atmospheric passage model uses neither a constant ablation

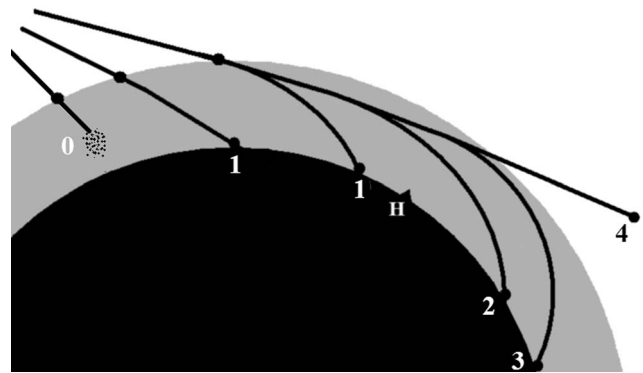


**Figure 2.** Possible trajectories for HSR- and BI-like meteoroids incident on Mars’ atmosphere. (0) “Burnup,” mass loss, due to ablation, down to a mass below 0.1 kg; (1) direct impact, forming a hypervelocity impact crater; (2) “over the horizon” impact trajectory; (3) “fallback” trajectory; and (4) an object that passes through the atmosphere, reemerges, and escapes the planet. “H” marks the horizon as viewed from the point of atmospheric entry.

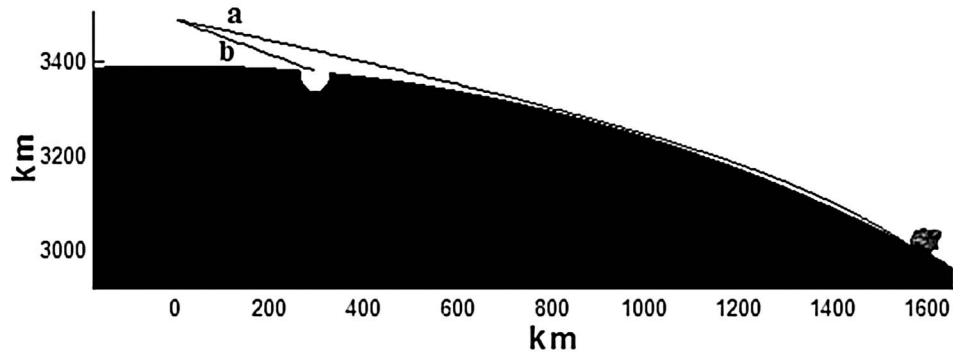


**Figure 3.** To-scale comparison of type 3 (“fallback,” line a) and type 1 (“direct,” line b) flight paths taken from the results of this study. Both started at  $11.0 \text{ km s}^{-1}$ . The fallback path is several times the length of the direct one and ends in a very shallow angle impact at less than  $1.8 \text{ km s}^{-1}$ , while the test object on the direct path impacts at  $\sim 6.5 \text{ km s}^{-1}$ . Thus, according to our criteria, object “a” dropped as a meteorite, while object “b” was destroyed, forming a hypervelocity impact crater.

coefficient ( $C_H$ ) nor a “flat Mars” approximation, both of which are common simplifications but inappropriate for use here. The ablation coefficient varies with atmospheric density and projectile speed by a factor of 10 or more [Bibermann *et al.*, 1980], and this variation is especially significant for the large ranges of velocities that are of greatest interest herein. Therefore, a  $C_H$  dependent on projectile speed and atmospheric density [Chappelow and Sharpton, 2006a] was constructed from results found in Bibermann *et al.* [1980] and implemented in the model in the form of a “look-up table.” The flat Mars approximation would only be appropriate if we could ignore the relatively rare atmosphere-grazing meteoroids. However, as will be shown, these grazing objects are exactly the ones of greatest interest for our purposes. A model that uses the flat Mars approximation cannot reproduce these. Also, aerial fragmentation was not included in the model, as previous results [Chappelow and Sharpton, 2005] indicate that this should be an exceedingly rare event in Mars’ current atmosphere.

## 5. Results and Discussion

[22] Results for HSR and BI are shown in Figures 5 and 6, respectively. We found that today’s martian atmosphere can account for the presence of both Heat Shield Rock and the Block Island meteorite, but only if they entered the atmosphere within very narrow, coupled limits of the entry parameters. The entry parameter ranges of interest (ROI) identified for both HSR and BI were  $50 \text{ kg} \leq m_o \leq 900 \text{ kg}$ ,  $6.0 \text{ km s}^{-1} \leq v_o \leq 20.0 \text{ km s}^{-1}$ , and  $9.50^\circ \leq \theta_o \leq 13.50^\circ$ . According to the velocity and entry angle distributions (Figures 4b and 4c), only 2.7%, or about 1 in 36, of all Mars-incident iron meteoroids fall within these entry velocity and angle ranges. Separate, specific limits for HSR and BI are given in Table 2. However, these limits are far from exclusive; the vast majority of iron meteoroids that do fall within them still do not produce meteorites but instead escape the atmosphere (if they enter too shallow) or impact destructively (if they enter too steep), as indicated on the figures.

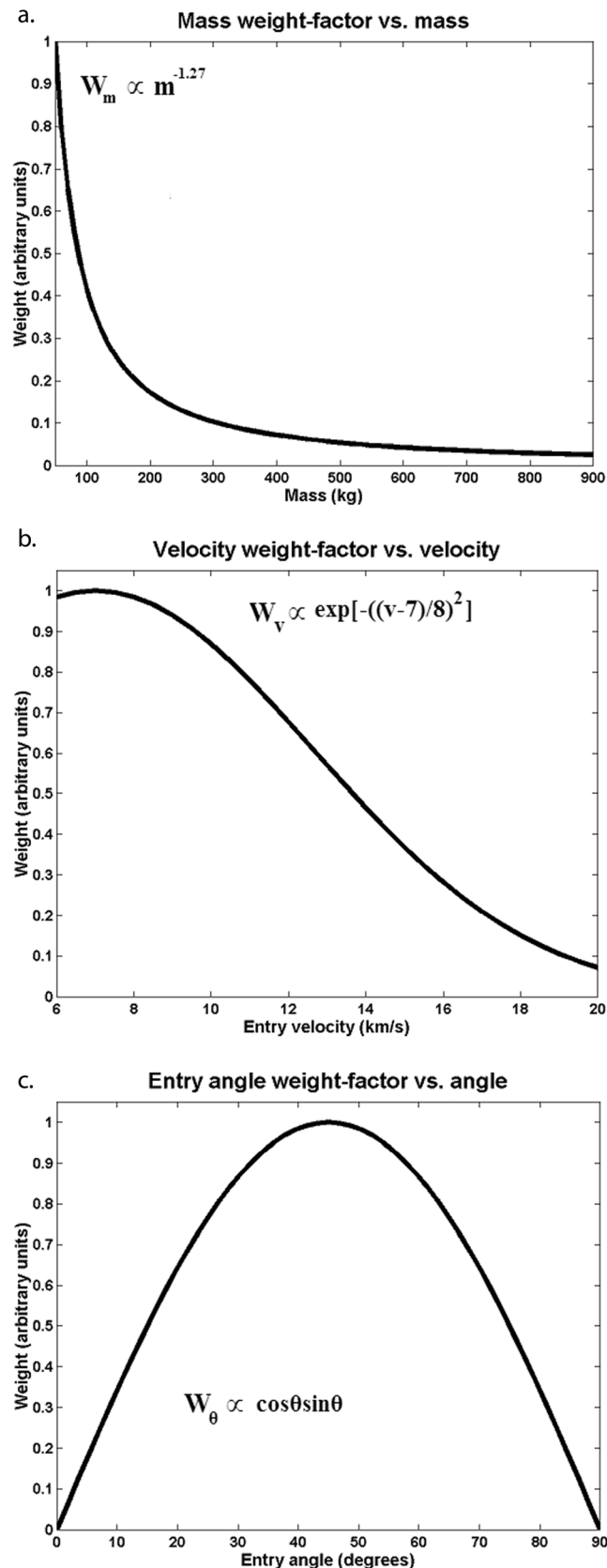
[23] All of the positive results for both HSR and BI followed over the horizon or fallback type trajectories on

their way through the atmosphere, a fact that has important implications for the possibility that the four iron meteorites so far discovered may represent a strewn field. These flight paths all end in impacts at very shallow angles (Table 2), which tend to favor the survival of meteorites and cause them to ricochet upon impact [e.g., Gault and Wedekind, 1978]. Given the strength of iron meteorites [Petrovic, 2001] and these low angle glancing impacts, iron meteorites should be able to survive impact velocities up to  $2 \text{ km s}^{-1}$  [see Chappelow and Sharpton, 2005, and references therein]. Ricochet may account for the absence of any evidence of their impacts nearby, such as impact pits, even if they arrived relatively recently.

[24] As shown on the figures, higher-speed projectiles must also have larger masses if they are to land as HSRs or BIs. This dependence, and the forms of the mass and velocity probability distributions, means that the probability of producing an HSR (or other iron meteorite) drops sharply with increasing velocity, and this is reflected in the figure. Thus, high-velocity projectiles are far less likely to land as meteorites than slower ones and must lose significant fractions of their masses to ablation in the process.

### 5.1. Heat Shield Rock

[25] Figure 5 shows that even meteoroids that fall within the ROI produce few HSR-sized meteorites; entry mass, velocity, and angle must all be just right, or they still impact destructively or escape Mars’ atmosphere. As a result, only 3.0% of iron meteoroids that fit within the ROI produce HSR like meteorites. And since the ROI itself includes only 2.7% of all possible entry angles and velocities, only 0.08% (or about 1 in 1210) of all 50–900 kg iron meteoroids incident on Mars drop as HSR meteorites. All of these arrive via over the horizon (48%) or fallback (52%) flight paths. Clearly the bulk of HSR-like meteorites on Mars will have entered the atmosphere at speeds less than about  $13 \text{ km s}^{-1}$ , at angles less than  $12.8^\circ$ , and with masses less than about 70 kg, unless they encountered a denser atmosphere. For speeds beyond  $20 \text{ km s}^{-1}$  the probability of producing an HSR drops to near zero.



## 5.2. Block Island

[26] Although BI is several times the mass of HSR, Figure 6 shows that even today's martian atmosphere can slow it enough to land as a meteorite. However, its entry conditions are considerably more restricted than those for HSR. Only 0.25% of iron meteoroids larger than 50 kg that fall within the ROI eventually land as BI like meteorites, and overall, only about 0.007% (1 in 14,500) 50 + kg iron meteoroids produce a BI-like meteorite. Over 80% of these follow fallback-type flight paths, proving that these kinds of flight paths are required to deposit the largest iron meteorites on Mars. Thus, as single falls, large irons must be quite rare on Mars.

[27] The fraction of BI-like meteorites (0.007%) compared to HSR-like ones (0.08%) indicates that we should expect many smaller (kilogram to tens of kilograms) iron meteorites for every BI found, for the assumed mass distribution. There should be approximately 11–12 HSRs for every BI, if they represent independent, single meteorite falls. Irons have been easy for Opportunity to detect because they stand out as dark-toned rocks, compared with the light-toned outcrop and basaltic sand, and according to these results, it should have discovered a number of smaller ones. But if so, where are these meteorites? Have geological processes hidden or destroyed them? Or were they sorted out during atmospheric passage?

[28] In view of the results for HSR and BI, there must also be an upper limit to the masses of iron meteorites that can be landed on Mars with the current atmosphere. Masses larger than this limit would require a denser atmosphere in order to impact at less than  $2 \text{ km s}^{-1}$ . The largest meteorite produced by our simulation was about 880 kg in mass, which must serve only as a lower limit to the maximum iron meteorite size, since our mass range of interest only went up to about 900 kg. However, this shows that Mars' current atmosphere may land iron meteorites considerably larger even than BI, given favorable entry conditions, although such events become increasingly improbable.

[29] Recently, *Beech and Coulson* [2010] used methods similar to those used here for essentially the same purpose. They concluded that BI could not have landed under present Mars atmospheric conditions but would have required an atmosphere 10–100 times denser. However, their results are strongly affected by a number of their assumptions and methods. These include (1) an estimate of 850 kg for the mass of BI; (2) use of a “flat Mars” approximation (no over the horizon flight paths); (3) an impact survival threshold velocity of  $1 \text{ km s}^{-1}$  rather than  $2 \text{ km s}^{-1}$  for iron meteor-

**Figure 4.** Graphs of the (a) mass, (b) velocity, and (c) entry angle probability distribution functions of meteoroids encountering Mars based on the derived impact rate and population of asteroids, after the derivation and discussion in *Chappelow and Sharpton* [2005]. The equation of each is given in the figure. The mass-frequency distribution is based on lunar cratering and other data. The velocity-frequency distribution is a half-Gaussian fit to data found in *Chyba* [1991] and the limits  $v_{\min} = 7 \text{ km s}^{-1}$  and  $v_{\max} = 31 \text{ km s}^{-1}$ . The entry angle frequency distribution is the standard sine-squared distribution.

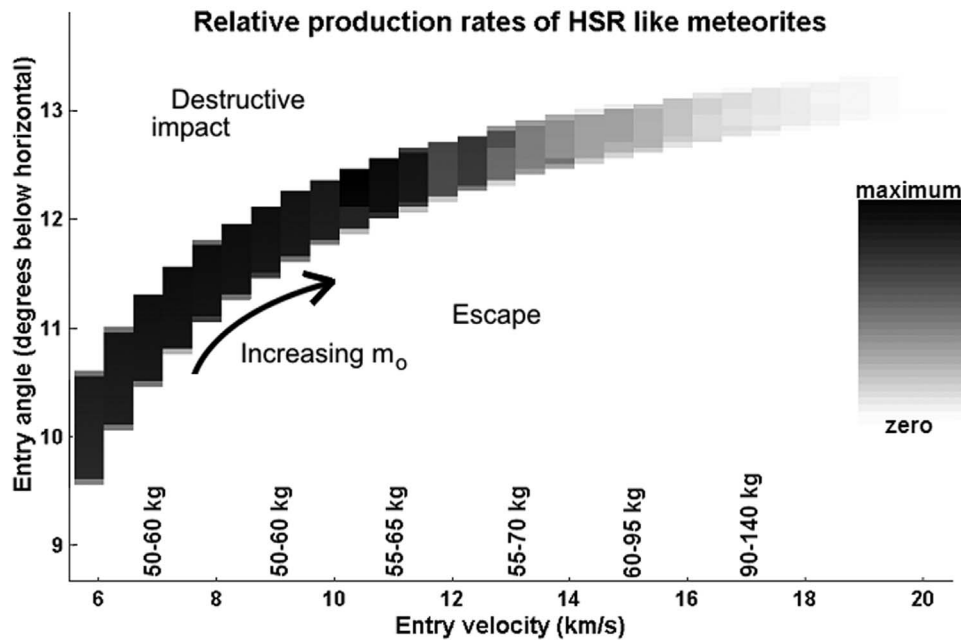


**Figure 5.** Relative contributions to the population of Heat Shield Rock-like iron meteorites versus entry angle and velocity. Relative contributions are shown in grayscale, where white is zero contribution and black is the maximum contribution (scale at right). Entry mass ranges are given along the bottom of the graph, as well as an arrow indicating trend, and outcomes other than meteorites are indicated on the figure as “escape” and “destructive impact.” Results show that it is possible to land HSR-like iron meteorites with the current atmosphere for entry angles of  $10^{\circ}$ – $13^{\circ}$  and entry velocities of  $6$ – $18$   $\text{km s}^{-1}$ . Some minor artifacts in the results between  $11$   $\text{km s}^{-1}$  and  $15$   $\text{km s}^{-1}$  are due to the necessity of using a logarithmic scale for the entry masses.

oids, largely deduced from the absence of a crater or pit under BI; and (4) investigation of only three sets of entry conditions ( $\nu_o = 11, 11, 5$   $\text{km s}^{-1}$ ;  $\theta_o = 42, 15, 15^{\circ}$ ), at least the first two of which correspond to very “direct” flight paths through the atmosphere and are unfavorable for producing meteorites. In contrast, our results show that landing massive iron meteorites on Mars is possible under current atmospheric conditions, but it requires shallower entries; long, over the horizon flight paths; and glancing ricochet landings that are survivable at higher velocities.

### 5.3. Comparison to Small Stony Meteorite Finds

[30] Along with the four irons, Opportunity has also discovered four small stony meteorite candidates (and related objects), three of which (“Santa Catarina,” “Santorini,” and “Kasos”) are between  $0.1$   $\text{kg}$  and  $10$   $\text{kg}$  in mass [Schröder *et al.*, 2010]. The entry condition ranges presented in that companion paper (and included in Table 2) show that the restrictions that apply to the irons addressed here do not apply to these lower density and much less massive stony meteorite candidates. Figure 7, which is adapted from that study, shows that these small stony meteorites should greatly outnumber the large irons that are the subject of the present study. Stony meteoroids also considerably outnumber irons in the asteroid belt [e.g., Tholen, 1989], so many more stony meteorites would be expected compared to iron meteorites. Yet only four small (and possibly associated) stony meteorite candidates have been found, and none of these approach the mass of the irons. Thus, the irons

appear to be greatly overrepresented relative to the stones among known and suspected large meteorites found by Opportunity.

[31] There are several possible reasons for this disparity. First, once on the surface, stones are more susceptible to mechanical erosion than irons, which would reduce both their numbers and sizes relative to the irons. However, both chemical and mechanical weathering of both stony and iron meteorites are expected to be extremely slow on Mars [Bland and Smith, 2000], even compared to very dry areas on Earth, given the near absence of liquid water and the lack of evidence for extreme eolian erosion of hard rocks at the landing sites on Mars (e.g., Ashley *et al.*, submitted manuscript, 2010). Thus, differential erosion and weathering seem less likely to account for the disparity between the numbers of stones and irons than other possibilities.

[32] Another possibility is a selection effect based on differences in detectability of iron versus stony meteorites, due to their differences in physical properties and outward appearance. However, although it is quite possible that some small stony meteorites have been missed by Opportunity during her traverse, it is unlikely that any large, dark-toned rocks have been missed. Surface materials observed at Meridiani are limited to light-toned sulfate outcrop, basaltic sand, and a population of small dark pebbles (generally centimeter sized) some of which may represent fragments of the stony impactor population [e.g., Golombek *et al.*, 2010]. Any large rock that differed from the local surface materials would have been detected by Opportunity and investigated.

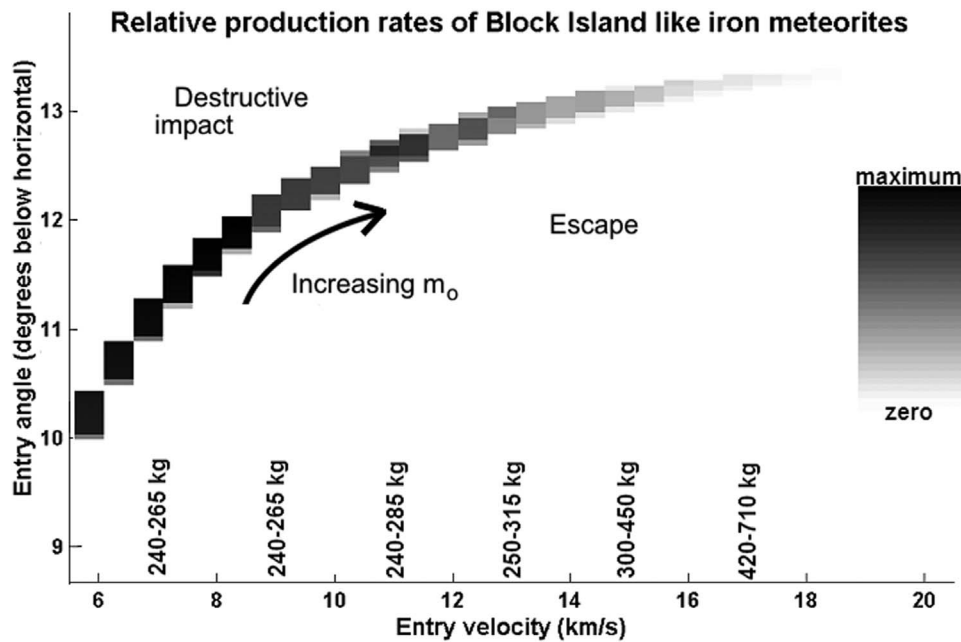


**Figure 6.** Relative contributions to the population of BI-like iron meteorites versus entry angle and velocity. Relative contributions are shown in grayscale, where white is zero contribution and black is the maximum contribution (scale at right). Entry mass ranges are given along the bottom of the graph, as well as an arrow indicating trend, and outcomes other than meteorites are indicated on the figure as “escape” and “destructive impact.” Results show that it is possible to land BI-like iron meteorites with the current atmosphere for entry angles of  $10^{\circ}$ – $13^{\circ}$  and entry velocities of  $6$ – $18$   $\text{km s}^{-1}$ , although such events are much less probable than HSR meteorites. Some minor artifacts in the results between  $11$   $\text{km s}^{-1}$  and  $14$   $\text{km s}^{-1}$  are due to the necessity of using a logarithmic scale for the entry masses.

No stony meteorites comparable in size to the irons have been discovered, so we can be reasonably sure they simply are not there to be found.

[33] A third possibility is that the stony meteorites break into small pieces, either in the atmosphere or when they hit the surface, since they are substantially weaker (by factors of approximately 4 to 20 times, in compressive strength) than iron meteorites [Petrovic, 2001]. The model results presented herein suggest that iron meteorites survive landing when they are slowed by the atmosphere on long, shallow entry paths. These shallow entries lead to very low angle impacts with the surface at velocities  $<2$   $\text{km s}^{-1}$ . The strong iron meteorites likely ricochet across the surface but survive intact, as indicated by the regmaglypted surfaces of the irons Opportunity has discovered. Stony meteorites are much weaker than intact irons and much more likely to break up on impact. Support for this hypothesis comes from the significant porosity of stony meteorites and the strong relation of increasing porosity with decreasing rock strength [e.g., Flynn *et al.*, 1999; Warren, 2001; Okubo, 2007].

[34] On the other hand, the density of stony meteorites is generally less than half that of iron, so they are decelerated more efficiently than irons (by a factor of approximately 1.75, assuming  $\rho_{\text{stone}} = 3300$   $\text{kg m}^{-3}$  and  $\rho_{\text{iron}} = 7900$   $\text{kg m}^{-3}$ ). Therefore, they impact the surface considerably slower than irons of equal mass, increasing their likelihood of survival. Which of these effects predominates is a question we have not yet investigated.

[35] Nevertheless, we suggest that breakup of stony meteorites on impact is a probable explanation for at least part of the excess of large (tens to hundreds of kilograms) iron meteorites compared to stones at Meridiani Planum. If this is correct, the population of small stony meteorites on Mars could accumulate from spallation during impact cratering as well as fracturing on glancing, low-angle impacts. The fragments of rocks associated with the stony meteorite Santa Catarina found around Victoria crater [Schröder *et al.*, 2010] could be a strewn field that resulted from either of these mechanisms.

[36] As mentioned above, it is also possible that the irons are numerous because they are part of a strewn field. If this is the case, they may in fact outnumber the stony meteorites, locally, even if the stones are also part of a separate strewn field or are spall or impact fragments from a larger stony object, as proposed by Schröder *et al.* [2010]. Indeed their angular shapes and lack of fusion crusts or regmaglypts suggest they may simply be surviving fragments of a larger object that shattered on impact [Schröder *et al.*, 2010].

**Table 2.** Meteorite Entry Conditions and Impact Angles

	Entry Mass (kg)	Entry Speed ( $\text{km s}^{-1}$ )	Entry Angle (deg)	Impact Angle (deg)
Heat Shield Rock	50–250	6.0–20.0	9.60–13.40	1.4–10.4
Block Island	250–800	6.0–18.5	10.00–13.40	2.3–8.5
Stones		6.0–17.0 <sup>a</sup>	8.0–39.0 <sup>a</sup>	

<sup>a</sup>From Schröder *et al.* [2010].



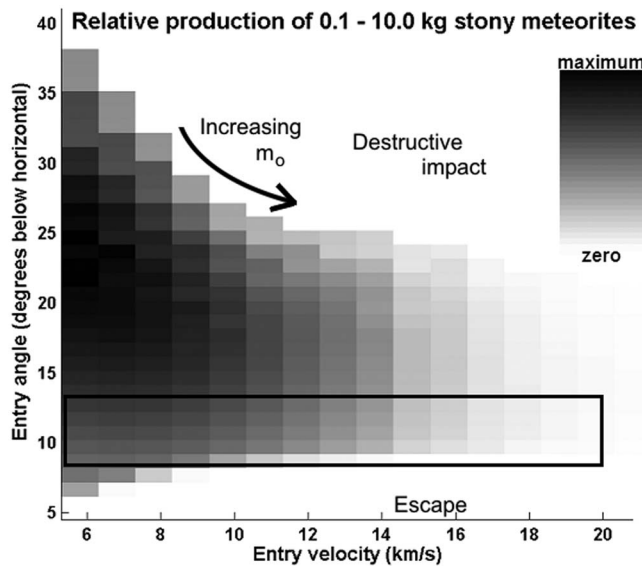


**Figure 7.** Relative contributions to the population of 0.1–10.0 kg stony meteorites versus entry angle and velocity (adapted from Schröder *et al.* [2010]). Relative contributions are shown in grayscale, where white is zero contribution and black is the maximum contribution (scale at right). Entry mass ranges are given along the bottom of the graph, as well as an arrow indicating trend, and outcomes other than meteorites are indicated on the figure as “escape” and “destructive impact.” The box roughly outlines the region in  $\nu_o - \theta_o$  space represented in Figures 5 and 6. Some minor artifacts are due to the necessity of using a logarithmic scale for the entry masses.

#### 5.4. Are the Iron Meteorites Part of a Strewn Field?

[37] It seems very improbable that four such similar iron meteorites (assuming all four are IABs [Fleischer *et al.*, 2010b]) can land in such a small area via four separate rare events, especially since no other types of irons have been found. The number found thus far, their compositional similarity, and their proximity to each other all suggest that they are parts of one larger object that broke up in the atmosphere and scattered fragments across the surface, forming a strewn field. In addition, the similarity in their masses and the absence of smaller iron meteorites (Table 1), suggests that they have been sorted, as would happen during a long, oblique atmospheric flight.

[38] However, the lack of fracture-related features and the ubiquity of regmaglypts on the meteorites, the high strength of meteoritic iron and low density of Mars’ atmosphere, and the 10 km of separation between the putative fragments all argue against this hypothesis. The regmaglypts indicate that fragmentation must have taken part early enough in the meteorites’ atmospheric flight for them to form, and for fractures to be erased, by ablation. However, if only direct trajectories are considered, this tends to imply a high-altitude fragmentation event, and the dynamic pressures at high altitudes would be extremely small compared to assumed strengths of iron meteorites. In fact, as noted above, Chappelow and Sharpton [2005] found that fragmentation

of iron meteoroids should be rare at any altitude, even in a martian atmosphere 10 times as dense as today’s.

[39] The dynamic pressures would also be too small to explain the scatter of the meteorites found on the surface, if the scattering is due to the aerodynamic side forces briefly applied to the fragments immediately after breakup [Passey and Melosh, 1980; Artemieva and Shuvalov, 2001]. These are the forces thought to be responsible for dispersing the fragments that form most of the crater clusters observed on Mars and other planets. Typically these clusters are formed by objects on ordinary direct trajectories that break up in the atmosphere and the fragments are given transverse accelerations by aerodynamic forces between them, which scatter them before impact. However, a calculation using equation (11) in Chappelow and Sharpton [2005] and some generous assumptions (e.g., breakup at the optimum altitude of two scale heights above the surface and a shallow entry angle of 15°) yields an estimate of only about 150 m for the maximum scatter of iron fragments via this mechanism. This amount of scatter is consistent with some of the crater clusters found on Mars [e.g., Popova *et al.*, 2003, 2007]. Analysis of crater clusters that have formed in the past 10 years (from before and after imaging [Malin *et al.*, 2006; Daubar *et al.*, 2010]) shows that these clusters require very weak and low-density impactors to scatter the craters by the observed several hundred meters [Ivanov *et al.*, 2008, 2009]. In addition, these objects still impact at high speeds, leaving craters rather than intact meteorites. Thus, fragmentation and scattering by this mechanism can account for neither the 10 km spread of the four iron meteorites Opportunity has located nor their survival of impact with the surface, if they constitute a strewn field.

[40] Thus, we are left with an apparently contradictory set of observations. Evidence supporting the hypothesis that the iron meteorites are part of a strewn field include:

[41] 1. At least three of the iron meteorites have been classified as IAB irons, and no other types of irons have been identified.

[42] 2. All four irons have been found within 10 km of each other and three within less than 1 km (Figure 1).

[43] 3. The apparent absence of smaller iron meteorites suggests that they may have been sorted during atmospheric passage.

[44] Items that suggest the meteorites represent independent falls include:

[45] 4. None of the meteorites have shape features that suggest fragmentation but are instead populated by well-developed regmaglypts indicative of atmospheric ablation.

[46] 5. Aerodynamic side forces alone cannot explain the observed 10 km of scatter of the meteorites, at least not for direct trajectories.

[47] 6. The strength of meteoritic iron is much higher than the dynamic pressures encountered in any of our simulations.

[48] 7. The degrees of weathering of the four meteorites are apparently not the same (e.g., Ashley *et al.*, submitted manuscript, 2010).

[49] We considered these contradictory observations in view of our new results. First, it is clear that the iron meteorites must have followed over the horizon-type trajectories to decelerate enough to survive impact. This is a completely different scenario than the crater cluster forming

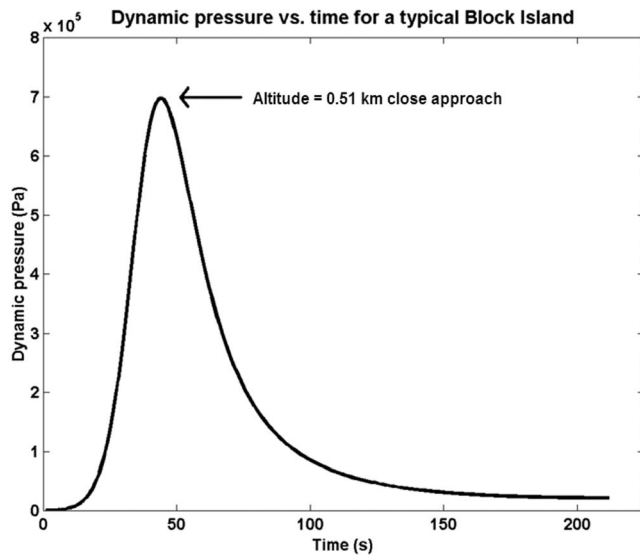


**Figure 8.** The dynamic pressure versus time on a typical Block Island meteoroid. The time of flight remaining after the dynamic pressure peak is over 2 min. The flight path is a type 3 (fallback) trajectory, and the peak is coincident with the first close approach to the surface, where in this case the dynamic pressure peaks at about 0.7 MPa.

events considered above, which followed direct trajectories. In addition to producing meteorites instead of craters, it introduces a mechanism that can account for their separation: differential drag deceleration (3D). In differential drag deceleration fragments of different masses undergo different degrees of deceleration, with smaller ones generally slowing faster and falling behind larger ones. If they are on extremely shallow (i.e., over the horizon-type) flight paths, the larger ones also land further downrange than small ones. In this way the fragments are both sorted and dispersed during atmospheric flight. The scattering effect is minimal for direct trajectories but, as will be shown next, can be quite large for over the horizon flight paths.

[50] To test whether this mechanism can account for the 10 km separation between HSR and BI, we sorted the HSR-like and BI-like outcomes from our results and compared the downrange flight distances of pairs of HSRs and BIs which share the same entry velocity and angle. This is equivalent to considering a single precursor object that fragments at 100 km altitude. Although this is an unrealistic assumption, it does establish an upper bound to the separation that may develop between the two putative fragments that eventually became HSR and BI. We found that BIs can carry up to tens or even hundreds of kilometers further downrange than their HSR counterparts, easily accounting for 10 km of separation. Thus, these indirect flight paths can account for both the low speed and impact angle and the fragment separation required to explain the meteorites as a strewn field. Sorting of the meteorites by size would also be a natural consequence of such an event.

[51] We found that the pairs that followed fallback-type flight paths were of particular interest. These objects encounter the denser lower atmosphere, and attendant maxima in dynamic pressure, early in their flights, then reascend for a while before finally falling back to the surface. If fragmentation

occurs at or near the dynamic pressure maximum, which occurs when the object makes its first close approach to the surface (Figure 8), the event would provide the long remaining flight times for regmaglypts to form and for fragment separation to occur. In fact, it would be possible that some of the original mass escaped back into space. This scenario would also explain the absence of smaller, kilogram-sized iron meteorites, given that the fragments would tend to be sorted during atmospheric flight. If this were the case, Opportunity would seem to have landed in the part of an elongated strewn field dominated by meteorites tens to hundreds of kilograms in mass, with smaller ones located in the uprange direction. The distribution of the meteorites (Figure 1), with the smallest, HSR (~50 kg), located about 9.6 km to the north-northeast of BI (~240 kg), and the intermediate SI and MI meteorites within 0.7 km to the west of BI, suggest that the flight path was from north-northeast.

[52] However, the maximum dynamic pressures encountered by any of the test objects (~1 MPa) are still far less than the estimated compressive strengths of meteoritic iron (hundreds of megapascals, for small samples [Petrovic, 2001]), which is consistent with previous results. Thus, we conclude that, while at this point, there is no dynamical reason to rule out the possibility of a strewn field, fragmentation of an iron meteoroid in Mars' current atmosphere remains a very unlikely event, unless that object were unusually fragile or prefractured prior to entry.

[53] Thus, while we have answered two of the major objections to the strewn field hypothesis and demonstrated a scenario of how it could happen that is consistent with most of the observations, the issue is still in doubt. The remaining objection, whether breakup could even occur, remains unanswered and will have to await further study.

## 6. Conclusions

[54] Current atmospheric conditions on Mars are sufficient to explain the presence of the four iron meteorites discovered by Opportunity, even the ~240 kg Block Island, although it requires unusual events to produce them. Only about 1 in 14,500, 220 + kg iron meteoroids entering Mars' atmosphere will land as a BI-like meteorite. We may expect about 12 HSR-sized iron meteorites for each BI-sized one found. Small stony meteorites, such as the four candidate rocks found to date, should be considerably more numerous than these irons, yet they have not been found in such numbers. And the four that *have* been found may actually be impact fragments of a single larger meteoroid that shattered upon impact, rather than individual falls.

[55] However, the improbability of four events independently dropping four IAB iron meteorites in the area explored by Opportunity raises the possibility that they are the result of a single aerial fragmentation event that dropped a strewn field. We have identified a scenario that answers some of the objections to this hypothesis, including how they soft-landed and how they could have been dispersed by at least 10 km. However, it still does not explain how Mars' thin atmosphere could fragment the original precursor iron meteoroid, unless that object were unusually fragile or prefractured prior to entry. Thus, whether these meteorites represent independent falls or a single event remains an open question.

[56] **Acknowledgments.** Research described in this paper was partially done by the MER project, Jet Propulsion Laboratory, California Institute of Technology, under a contract with the National Aeronautics and Space Administration. We appreciate comments provided by the MER science team and an anonymous reviewer.

## References

- Artemieva, N. A., and V. V. Shuvalov (2001), Motion of a fragmented meteoroid in the planetary atmosphere, *J. Geophys. Res.*, *106*, 3297–3309, doi:10.1029/2000JE001264.
- Beech, M., and I. M. Coulson (2010), The making of martian meteorite Block Island, *Mon. Not. R. Astron. Soc.*, *404*, 1457–1463, doi:10.1111/j.1365-2966.2010.16350.x.
- Biberman, L. M., S. Y. Bronin, and M. V. Brykin (1980), Moving of a blunt body through the dense atmosphere under conditions of severe aerodynamic heating and ablation, *Acta Astronaut.*, *7*, 53–65, doi:10.1016/0094-5765(80)90116-2.
- Bland, P. A., and T. B. Smith (2000), Meteorite accumulations on Mars, *Icarus*, *144*, 21–26, doi:10.1006/icar.1999.6253.
- Chappelow, J. E., and V. L. Sharpton (2005), Influences of atmospheric variations on Mars's record of small craters, *Icarus*, *178*, 40–55, doi:10.1016/j.icarus.2005.03.010.
- Chappelow, J. E., and V. L. Sharpton (2006a), Atmospheric variations and meteorite production on Mars, *Icarus*, *184*, 424–435, doi:10.1016/j.icarus.2006.05.013.
- Chappelow, J. E., and V. L. Sharpton (2006b), The event that produced heat shield rock and its implications for the Martian atmosphere, *Geophys. Res. Lett.*, *33*, L19201, doi:10.1029/2006GL027556.
- Chyba, C. F. (1991), Terrestrial mantle siderophiles and the lunar impact record, *Icarus*, *92*, 217–233, doi:10.1016/0019-1035(91)90047-W.
- Daubar, I. J., A. S. McEwen, S. Byrne, C. M. Dundas, M. Kennedy, and B. A. Ivanov (2010), The current martian cratering rate, *Proc. Lunar Planet. Sci. Conf.* [CD-ROM], *41*, 1978.
- Davis, P. M. (1993), Meteoroid impacts as seismic sources on Mars, *Icarus*, *105*, 469–478, doi:10.1006/icar.1993.1142.
- Fleischer, I., G. Klingelhöfer, C. Schröder, D. Mittlefehldt, R. V. Morris, M. Golombek, and J. W. Ashley (2010a), In situ investigation of iron meteorites at Meridiani Planum, Mars, *Proc. Lunar and Planet. Sci. Conf.* [CD-ROM], *41*, 1791.
- Fleischer, I., et al. (2010b), Mineralogy and chemistry of cobbles at Meridiani Planum, Mars, investigated by the Mars Exploration Rover Opportunity, *J. Geophys. Res.*, *115*, E00F05, doi:10.1029/2010JE003621.
- Flynn, G. J., L. B. Moore, and W. Klock (1999), Density and porosity of stone meteorites: Implications for the density, cratering, and collisional disruption of asteroids, *Icarus*, *142*, 97–105, doi:10.1006/icar.1999.6210.
- Gault, D. E., and J. A. Wedekind (1978), Experimental studies of oblique impact, *Proc. Lunar Planet. Sci. Conf.*, *9*, 3845–3875.
- Golombek, M., K. Robinson, A. McEwen, N. Bridges, B. Ivanov, L. L. Tornabene, and R. Sullivan (2010), Constraints on ripple migration at Meridiani Planum from Opportunity and HiRISE observations of fresh craters, *J. Geophys. Res.*, doi:10.1029/2010JE003628, in press.
- Ivanov, B. A. (2008), Small impact crater clusters in high resolution HiRISE images, *Proc. Lunar Planet. Sci. Conf.* [CD-ROM], *39*, 1221.
- Ivanov, B. A. (2009), Small impact crater clusters in high resolution HiRISE images: II, *Proc. Lunar Planet. Sci. Conf.* [CD-ROM], *40*, 1410.
- Johnson, J. R., K. E. Herkenhoff, J. F. Bell III, W. H. Farrand, J. Ashley, C. Weitz, and S. W. Squyres (2010), Pancam visible/near-infrared spectra of large Fe-Ni meteorites at Meridiani Planum, Mars, *Proc. Lunar Plan. Sci. Conf.* [CD-ROM], *41*, 1974.
- Maki, J. N., et al. (2003), Mars Exploration Rover engineering cameras, *J. Geophys. Res.*, *108*(E12), 8071, doi:10.1029/2003JE002077.
- Malin, M. C., K. S. Edgett, L. V. Posiolova, S. M. McColley, and E. Z. Noe Dobra (2006), Present-day impact cratering rate and contemporary gully activity on Mars, *Science*, *314*, 1573–1577, doi:10.1126/science.1135156.
- Melosh, H. J. (1989), *Impact Cratering: A Geologic Process*, 1st ed., Oxford Univ. Press, New York.
- Morris, R. V., et al. (2006), Mössbauer mineralogy of rock, soil, and dust at Meridiani Planum, Mars: Opportunity's journey across sulfate rich outcrop, basaltic sand and dust, and hematite lag deposits, *J. Geophys. Res.*, *111*, E12S15, doi:10.1029/2006JE002791.
- Okubo, C. H. (2007), Strength and deformability of light-toned layered deposits observed by MER Opportunity: Eagle to Erebus craters, Mars, *Geophys. Res. Lett.*, *34*, L20205, doi:10.1029/2007GL031327.
- Paige, D. A., M. P. Golombek, J. N. Maki, T. J. Parker, L. S. Crumpler, J. A. Grant, and J. P. Williams (2007), MER small crater statistics: Evidence against recent quasi-periodic climate variations, paper presented at the 7th International Conference on Mars, Pasadena, Calif., 9–13 July.
- Passy, Q. R., and H. J. Melosh (1980), Effects of atmospheric breakup on crater field formation, *Icarus*, *42*, 211–233, doi:10.1016/0019-1035(80)90072-X.
- Petrovic, J. J. (2001), Review: Mechanical properties of meteorites and their constituents, *J. Mater. Sci.*, *36*, 1579–1583, doi:10.1023/A:1017546429094.
- Popova, O. P., I. V. Nemtchinov, and W. K. Hartmann (2003), Bolides in the present and past martian atmosphere and effects on cratering processes, *Meteorit. Planet. Sci.*, *38*, 905–925, doi:10.1111/j.1945-5100.2003.tb00287.x.
- Popova, O. P., W. K. Hartmann, I. V. Nemtchinov, D. C. Richardson, and D. C. Berman (2007), Crater clusters on Mars: Shedding light on martian ejecta launch conditions, *Icarus*, *190*, 50–73, doi:10.1016/j.icarus.2007.02.022.
- Roberts, W. L., T. J. Thomas, and G. R. Rapp (1990), *Encyclopedia of Minerals*, 2nd ed., Chapman and Hall, New York.
- Schröder, C., et al. (2008), Meteorites on Mars observed with the Mars Exploration Rovers, *J. Geophys. Res.*, *113*, E06S22, doi:10.1029/2007JE002990.
- Schröder, C., et al. (2010), Properties and distribution of paired candidate stony meteorites at Meridiani Planum, Mars, *J. Geophys. Res.*, doi:10.1029/2010JE003616, in press.
- Tholen, D. J. (1989), Asteroid taxonomy classifications, in *Asteroids II*, edited by R. P. Binzel, T. Gehrels, and M. S. Mathews, pp. 1139–1150, Univ. of Ariz. Press, Tucson.
- Vasavada, A. R., T. J. Milavec, and D. A. Paige (1993), Microcraters on Mars: Evidence for past climate variations, *J. Geophys. Res.*, *98*, 3469–3476.
- Warren, P. H. (2001), Porosities of lunar meteorites: Strength, porosity, and petrologic screening during the meteorite delivery process, *J. Geophys. Res.*, *106*, 10,101–10,111, doi:10.1029/2000JE001283.

J. E. Chappelow, SAGA Inc., 1148 Sundance Loop, Fairbanks, AK 99709, USA. (john.chappelow@saga-inc.com)

M. P. Golombek, Jet Propulsion Laboratory, California Institute of Technology, Mail Stop 183-501, 4800 Oak Grove Dr., Pasadena, CA 91109, USA.